Residual ion tracking in ThomX

Danylo Radevych[1], Alexis Gamelin[2], Christelle Bruni[2]

1 - Taras Shevchenko National University of Kyiv (Ukraine)
2 - Laboratoire de l'Accélérateur Linéaire

Origin of ions in the pipeline

- Vacuum is not ideal ($p_0 \approx 3.06 \cdot 10^{-8}$ Pa).
- Ionization of the residual gas by electron bunch.
- Created ions are trapped in the beam's space charge potential.

III effects [1]

- Reduced beam lifetime (increased pressure).
- Emittance growth.
- Losses through excitation of resonances.
- Coherent beam instabilities.

[1] A. Poncet, "Ion trapping and clearing."

Interaction with the beam

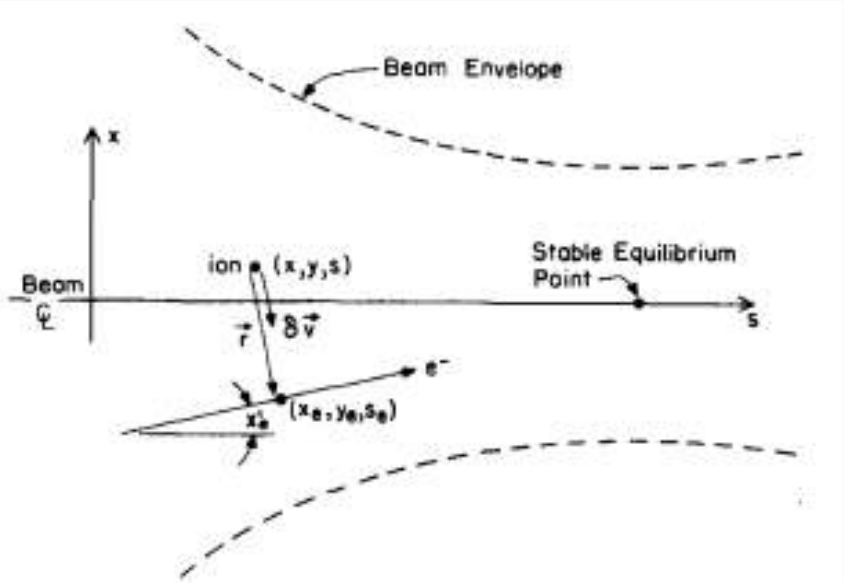

Figure 1: The force on an ion from an electron.

$$\delta\vec{v} = \frac{K}{r^2}\vec{r}. \qquad (1)$$

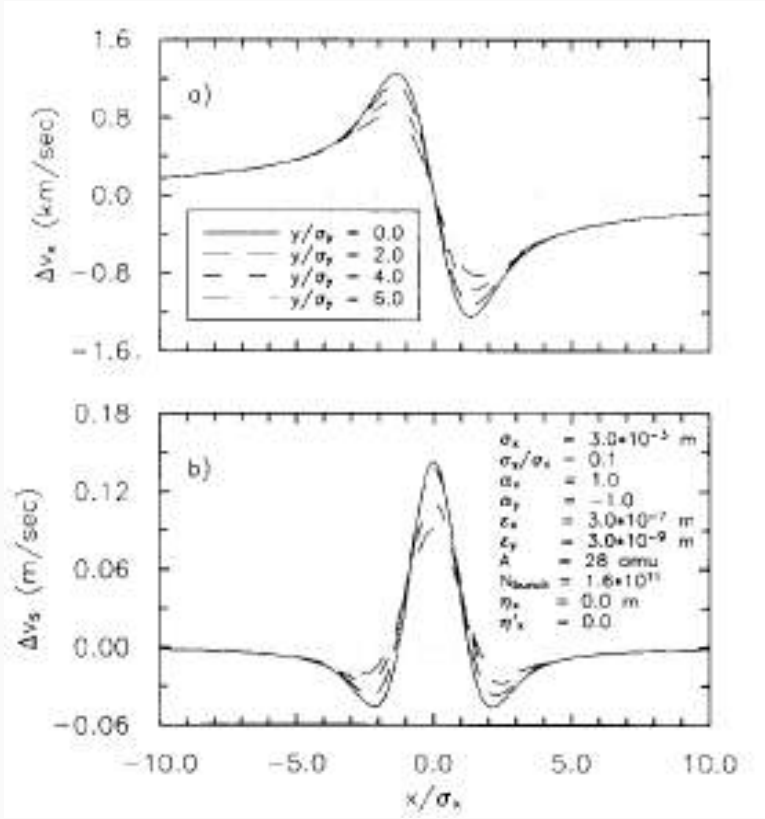

Figure 2: The variation of (a) horizontal kick Δv_x, and (b) the longitudinal kick Δv_s.

Taken from D. Sagan, "Some aspects of the longitudinal motion of ions in electron storage rings."

Interaction with the beam

Was implemented by Christelle Bruni and Alexis Gamelin.

Bassetti-Erskine:

$$\Delta v_y + i\Delta v_x = \sqrt{\frac{\pi}{2\left({\sigma_x}^2 - {\sigma_y}^2\right)}} N_e K \times \\ \times \left[w\left(\frac{x + iy}{\sqrt{2\left({\sigma_x}^2 - {\sigma_y}^2\right)}} \right) - e^{\left(-\left(\frac{x^2}{2{\sigma_x}^2} + \frac{y^2}{2{\sigma_y}^2} \right) \right)} w\left(\frac{x\frac{\sigma_y}{\sigma_x} + iy\frac{\sigma_x}{\sigma_y}}{\sqrt{2\left({\sigma_x}^2 - {\sigma_y}^2\right)}} \right) \right]. \tag{2}$$

Sagan:

$$\Delta v_s = \left[-\alpha_x \varepsilon_x + \left(\eta \tilde{\sigma_\varepsilon}\right)\left(\eta' \tilde{\sigma_\varepsilon}\right) \right] \frac{\partial \Delta v_x}{\partial x} - \alpha_y \varepsilon_y \frac{\partial \Delta v_y}{\partial y}. \tag{3}$$

- Ions' rapid transverse oscillations tend to cancel the effect of the transverse kicks.
- The effect of the kicks Δv_s is 3 orders below Δv_x or Δv_y.
- It can accumulate over a relatively long time scales.

Electrodes

$$\begin{cases} \dot{x} &= v_x, \\ \dot{y} &= v_y, \\ \dot{s} &= v_s, \\ \dot{v}_x &= \dfrac{q}{m} E_x, \\ \dot{v}_y &= \dfrac{q}{m} E_y, \\ \dot{v}_s &= 0. \end{cases} \quad (4)$$

1.5 and 2 times increase did not change the number of cleared ions.

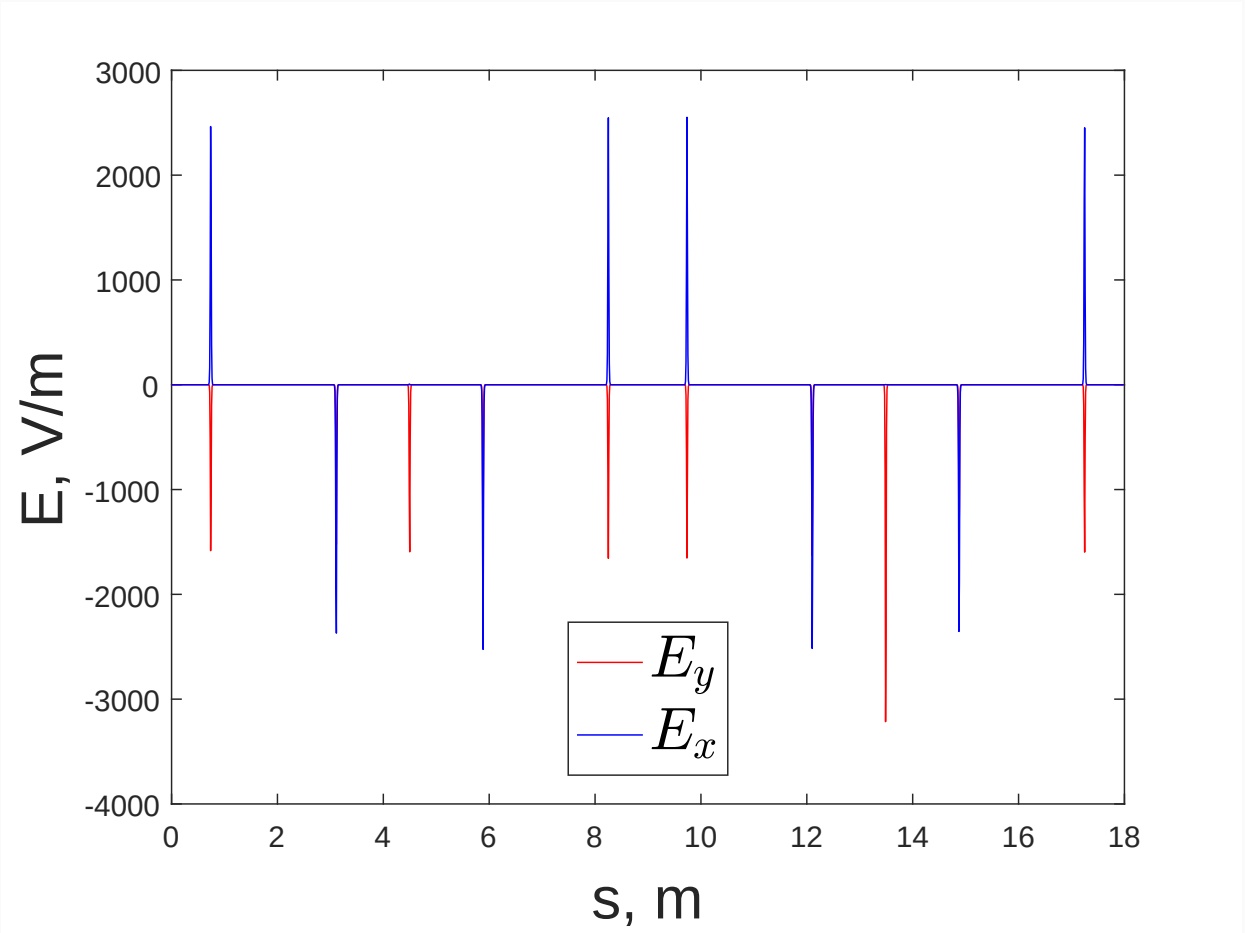

Figure 3: Electric field vs. longitudinal coordinate for one of the ThomX configurations.

Curvilinear frame

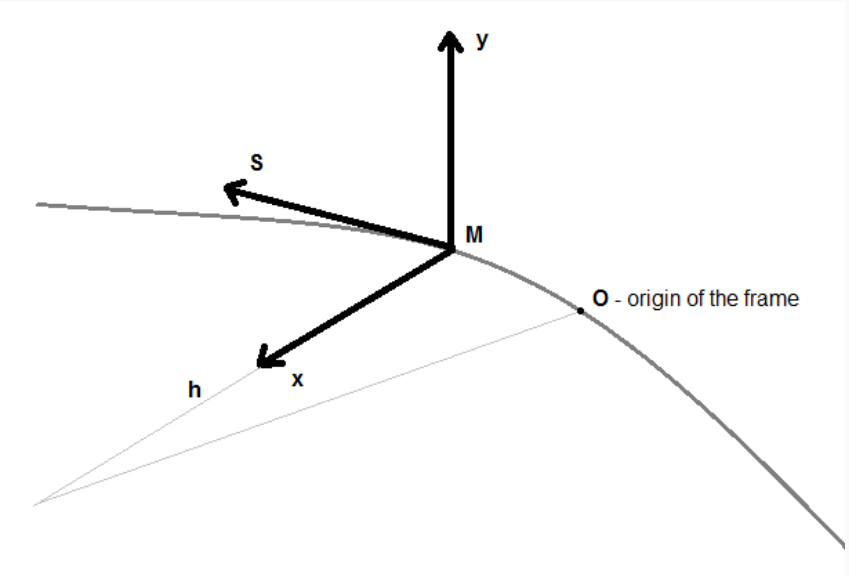

Figure 4: Curvilinear frame.

$h = \frac{1}{\rho(s)}$ – the parameter of a curve
$\rho(s)$ is the radius of curvature

Axis rotation:

$$\begin{cases} \dfrac{d\vec{x}}{ds} = -\dfrac{\vec{s}}{\rho} = -h\vec{s}, \\ \dfrac{d\vec{s}}{ds} = \dfrac{\vec{x}}{\rho} = h\vec{x}, \\ \dfrac{d\vec{y}}{ds} = 0. \end{cases} \tag{5}$$

$$\begin{cases} \dfrac{d\vec{x}}{dt} = \dfrac{d\vec{x}}{ds}\dot{s} = -h\dot{s}\vec{s}, \\ \dfrac{d\vec{s}}{dt} = \dfrac{d\vec{s}}{ds}\dot{s} = h\dot{s}\vec{x}, \\ \dfrac{d\vec{y}}{dt} = 0. \end{cases} \tag{6}$$

Equation of motion in the dipole magnetic field

$v_s \neq \dot{s},\ \dot{s} = \frac{v_s}{1-hx}$.

$$
\begin{cases}
\dot{x} &= v_x, \\
\dot{y} &= v_y, \\
\dot{s} &= \dfrac{v_s}{1 - \frac{eB_y}{p_e}x}, \\
\dot{v}_x &= -v_s \dfrac{q}{m} B_y - \dfrac{{v_s}^2}{\underbrace{\frac{p_e}{eB_y}}_{\rho} - x}, \\
\dot{v}_y &= 0, \\
\dot{v}_s &= v_x \dfrac{q}{m} B_y + \dfrac{v_x v_s}{\underbrace{\frac{p_e}{eB_y}}_{\rho} - x}.
\end{cases}
\tag{7}
$$

On the straight sections:

$\rho \to \infty$ - the same equations as in the ordinary Cartesian frame.

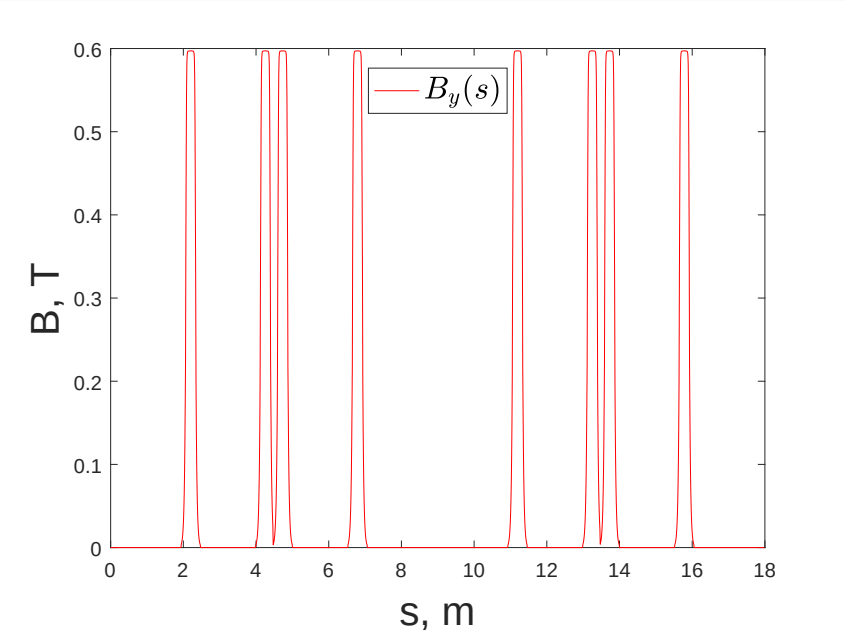

Figure 5: Dipole magnetic field vs. longitudinal coordinate.

Equation of motion in the quadrupole magnetic field

$$
\begin{aligned}
B_x &= -gy, \\
B_y &= -gx, \\
k &= \frac{g}{p_e/e}.
\end{aligned}
\tag{8}
$$

$$
\begin{cases}
\dot{x} &= v_x, \\
\dot{y} &= v_y, \\
\dot{s} &= v_s, \\
\dot{v}_x &= g\dfrac{q}{m}\Big(v_s x\Big), \\
\dot{v}_y &= -g\dfrac{q}{m}\Big(v_s y\Big), \\
\dot{v}_s &= g\dfrac{q}{m}\Big(-v_x x + v_y y\Big).
\end{cases}
\tag{9}
$$

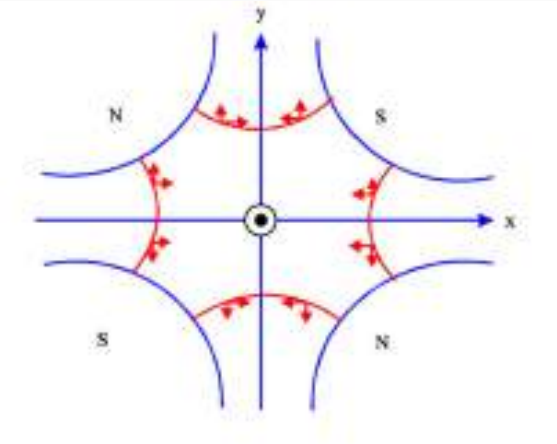

Figure 6: Axis directions inside a quadrupole magnet. **Taken from A. Latina, "Introduction to Transverse Beam Dynamics."**

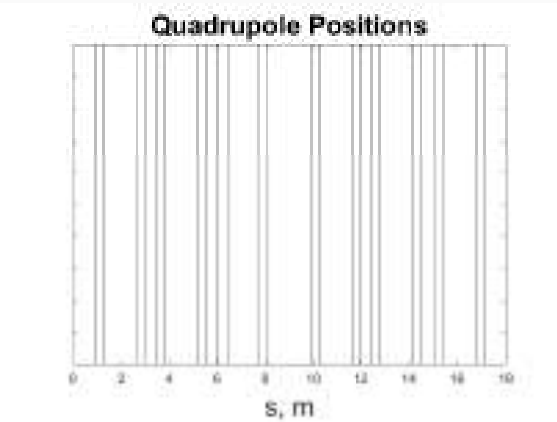

Figure 7: Quadrupole center positions along the ThomX ring.

Kickmap

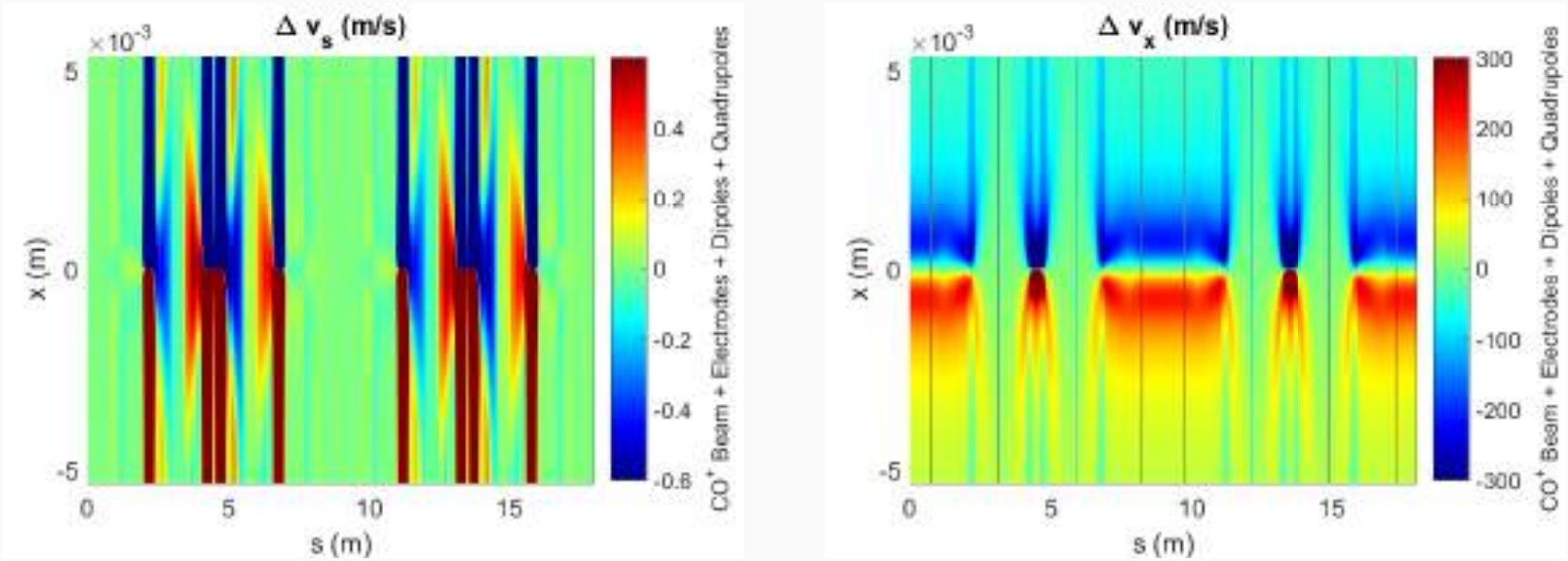

Figure 8: Kickmap for CO^+.

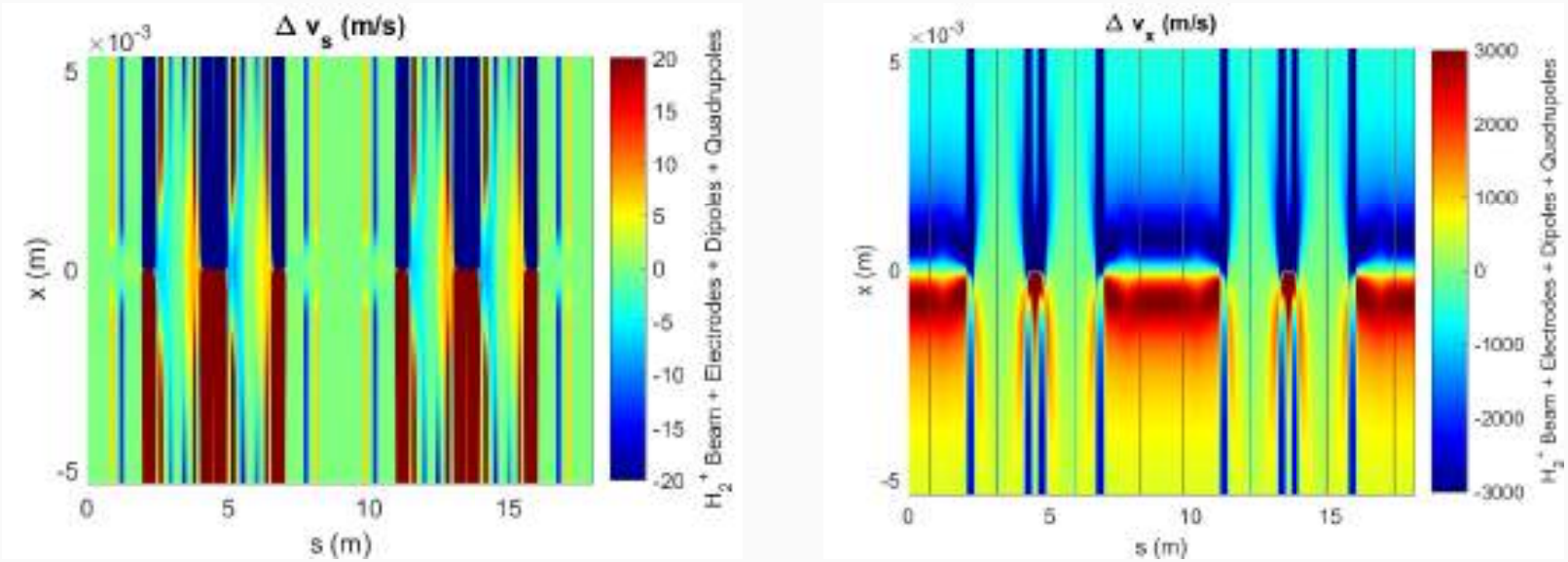

Figure 9: Kickmap for $H_2{}^+$.

From uniform to stable zones CO^+ ($4 \cdot 10^5$ turns)

Initial number of ions 25 000. 9 413 at the end of the cycle.

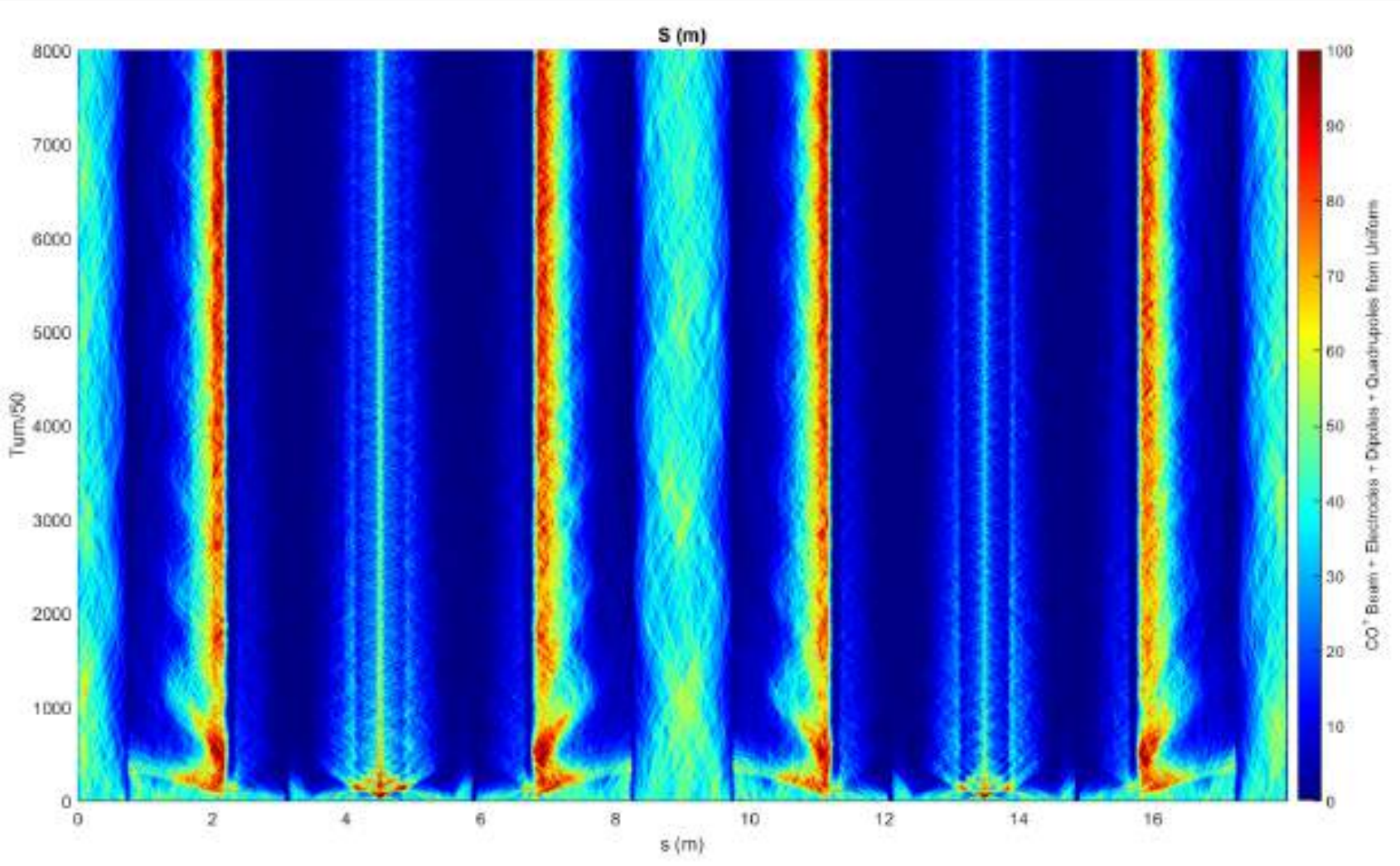

Figure 10: Longitudinal distribution of CO^+ ions. Initial distribution is uniform.

From uniform to stable zones $H_2{}^+$ ($4 \cdot 10^5$ turns)

Initial number of ions 25 000. 8 146 at the end of the cycle.

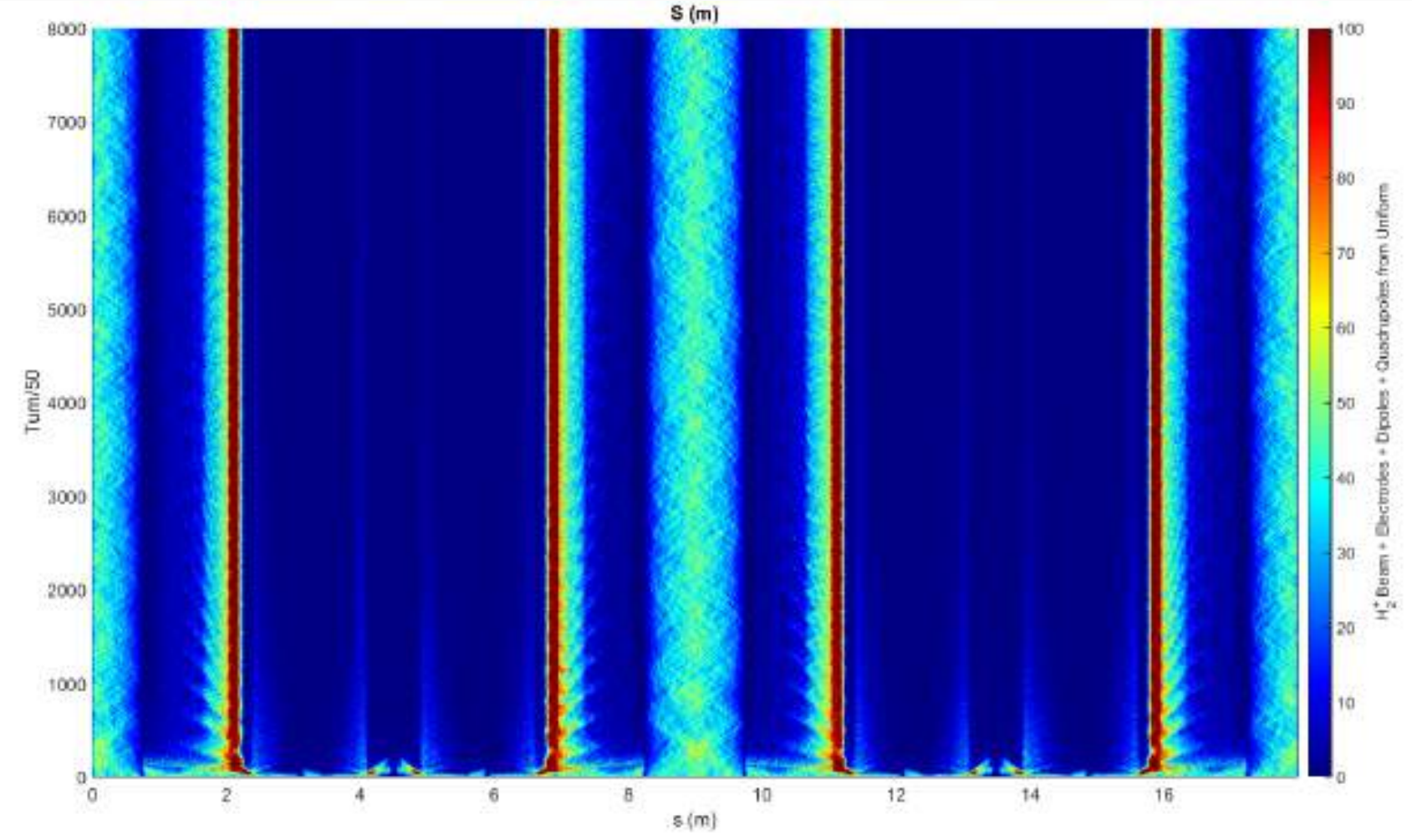

Figure 11: Longitudinal distribution of $H_2{}^+$ ions. Initial distribution is uniform.

Final turn

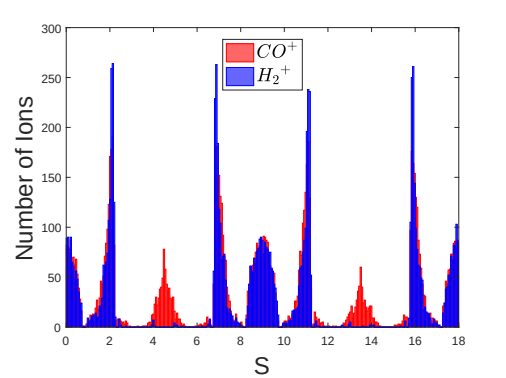

Figure 12: Longitudinal distribution of CO^+ and $H_2{}^+$ ions after $4 \cdot 10^5$ turns from uniform distribution.

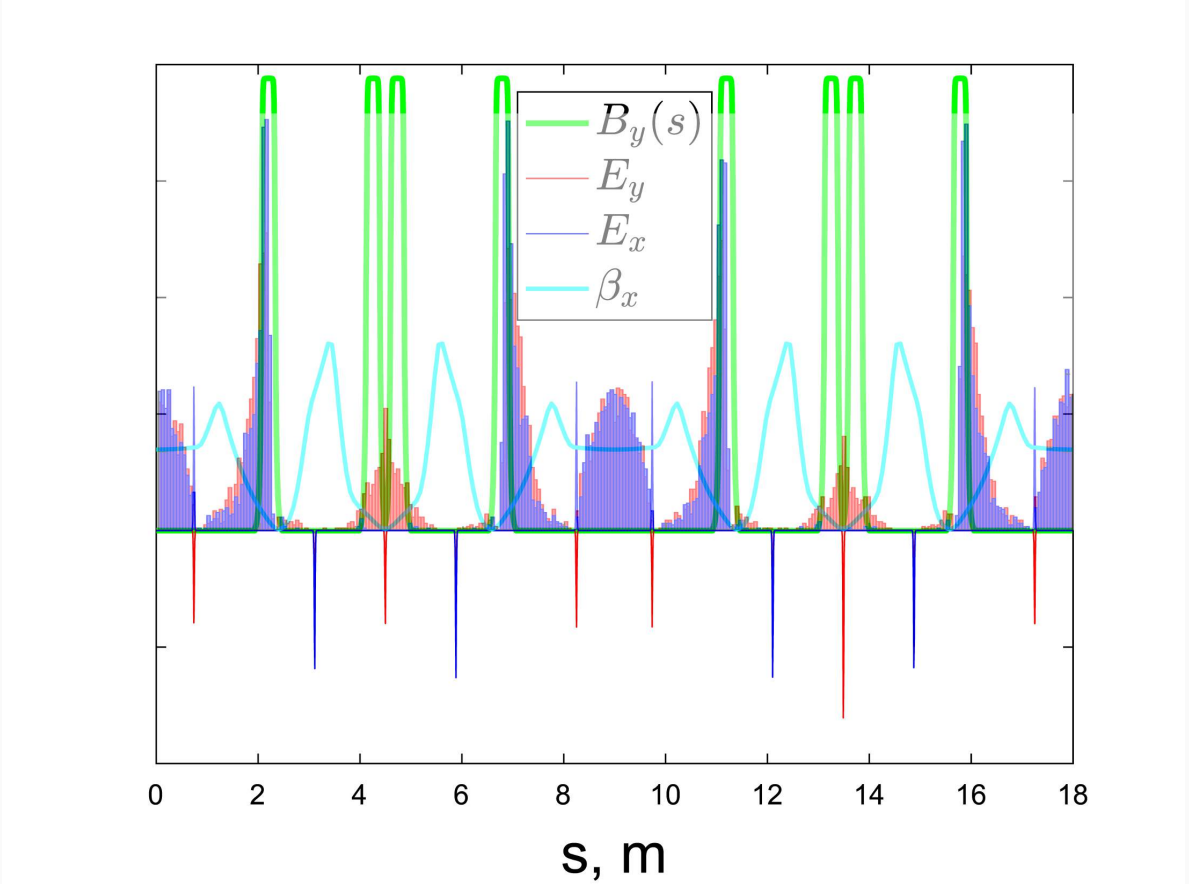

Figure 13: Fig. **??** with the behaviour of B_y, $E_{x,y}$, β_x.

Ions in dipoles

Actually, only 43% of survived ions.

Clearing coefficient from simulation

- $N_0 = N_{ions}(0)$ at the start of simulation.
- $N_{ions}(n)$ at the n^{th} turn.

$$\varepsilon(n) = \frac{N_{ions}(n)}{N_0}. \tag{10}$$

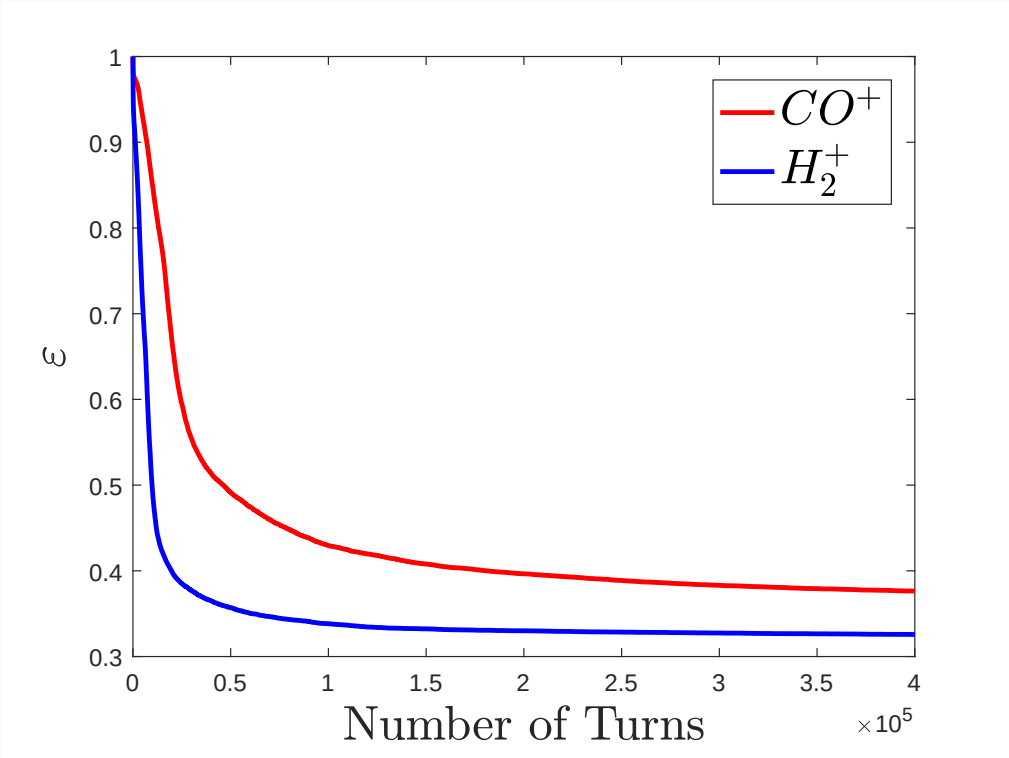

Figure 14: Clearing coefficient for the ions CO^+ and ${H_2}^+$ that were initially uniformly distributed along the ring.

Ions created during the one turn

- Molecules CO and H_2 are distributed uniformly along the ring.
- Pressure in the pipeline is $p_0 \approx 3.06 \cdot 10^{-8}$ Pa.
- Partial pressure: $p_{CO} \approx 0.1 \cdot p_0$, and $p_{H_2} \approx 0.9 \cdot p_0$.
- Ionization cross-section [2]:

$$\sigma^i = 4\pi \left(\frac{\hbar}{m_e c}\right)^2 \left\{ M^2 \left[\frac{1}{{\beta_e}^2} ln\left(\frac{{\beta_e}^2}{1-{\beta_e}^2}\right) - 1\right] + \frac{C}{{\beta_e}^2} \right\}. \quad (11)$$

Molecule	M^2	C	Z	A
H_2	0.5	8.1	2	2
CO	3.7	35.1	14	28

Table 1: Value of the M^2 and C constants for calculation of ionization cross-section.

- The number of created ions per turn: $N_{new}^{CO^+} \approx 10$, and $N_{new}^{{H_2}^+} \approx 17$.

[2] Y. Baconnier, A. Poncet, and P.F. Tavares, "Neutralisation of accelerator beams by ionisation of the residual gas."

First cycle ($4 \cdot 10^5$ turns, or 24 ms)

- At the start, $\varepsilon_{CO^+} = \varepsilon_{H_2{}^+} = 1$:
  $N_{ions}(0) = N_{new} \cdot \varepsilon(0)$.
- After the first turn, this number is reduced to $N_{new} \cdot \varepsilon(1)$ (function $\varepsilon(n)$ is decreasing). Also $N_{new} = N_{new} \cdot \varepsilon(0)$ new ions that were created during the first turn:
  $N_{ions}(1) = N_{new} \cdot \varepsilon(0) + N_{new} \cdot \varepsilon(1)$.
- After the second turn:
  $N_{ions}(2) = N_{new} \cdot \varepsilon(0) + N_{new} \cdot \varepsilon(1) + N_{new} \cdot \varepsilon(2)$.
  ...
- n^{th} turn:
  $N_{ions}(n) = N_{new} \cdot \varepsilon(0) + N_{new} \cdot \varepsilon(1) + N_{new} \cdot \varepsilon(2) + ... + N_{new} \cdot \varepsilon(n)$.

Integral

$$N_{ions}(n) = N_{new} \cdot \int_0^n \varepsilon(z)dz. \tag{12}$$

First cycle ($4 \cdot 10^5$ turns, or 24 ms)

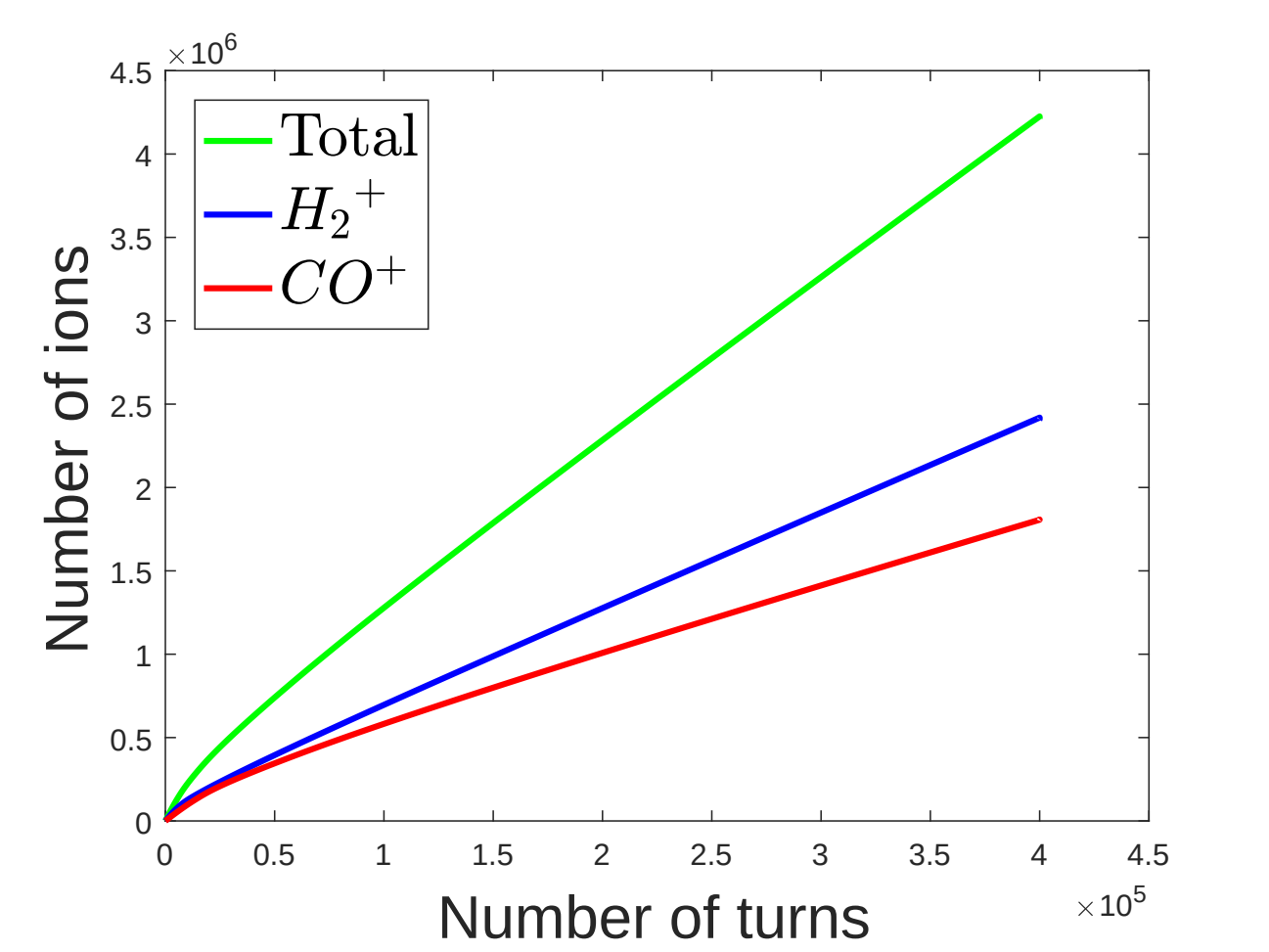

Figure 15: Number of ions CO^+ and $H_2{}^+$ that were initially uniformly distributed along the ring.

Small gap (66 turns, or 4 μs)

Does not clear CO^+ ions, but rather changes their transverse distribution.

- New ions are not created (no beam).
- Initial number of alive ions N_a is taken from the end of the previous part.
- Different clearing coefficient $\varepsilon_{sg}(n)$:

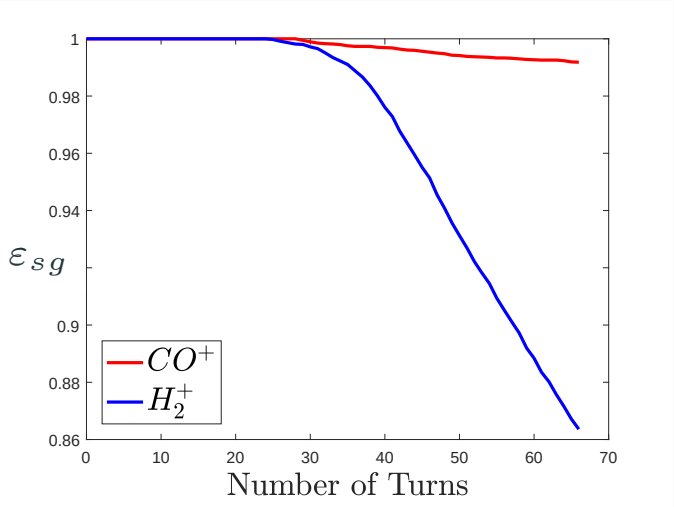

Figure 16: Clearing coefficient for the ions CO^+ and $H_2{}^+$ during the small gap.

Formula

$$N_{ions}(n) = N_a \cdot \varepsilon_{sg}(n), \quad n \in [0,\ n_{sg} = 66 \text{ turns}]. \tag{13}$$

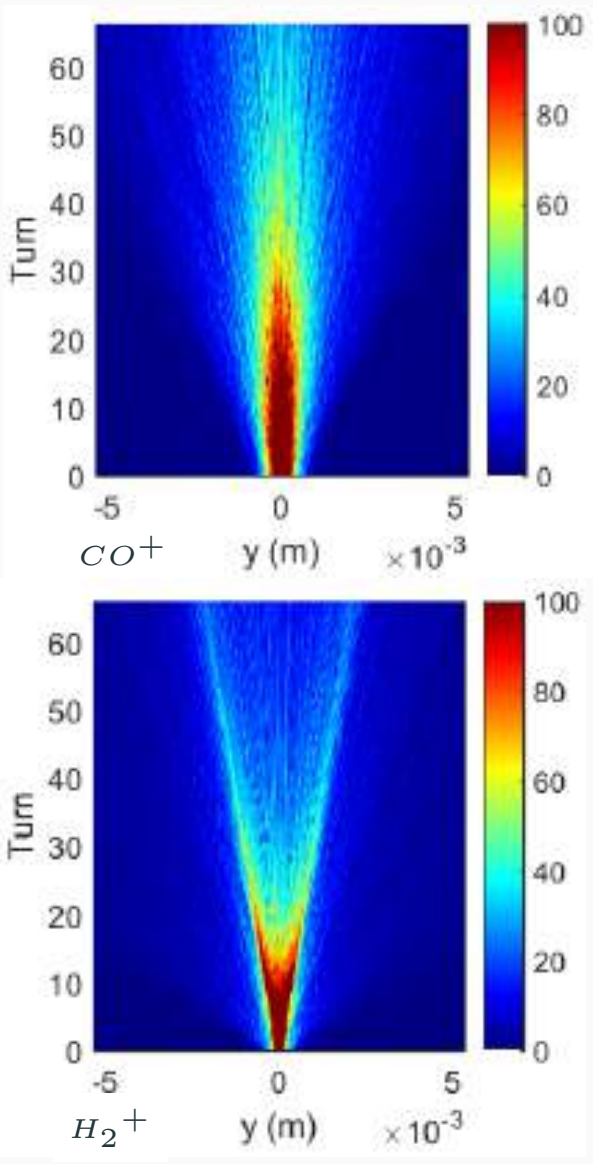

Figure 17: Transverse distribution of CO^+ and $H_2{}^+$ ions during the small gap.

First cycle and small gap

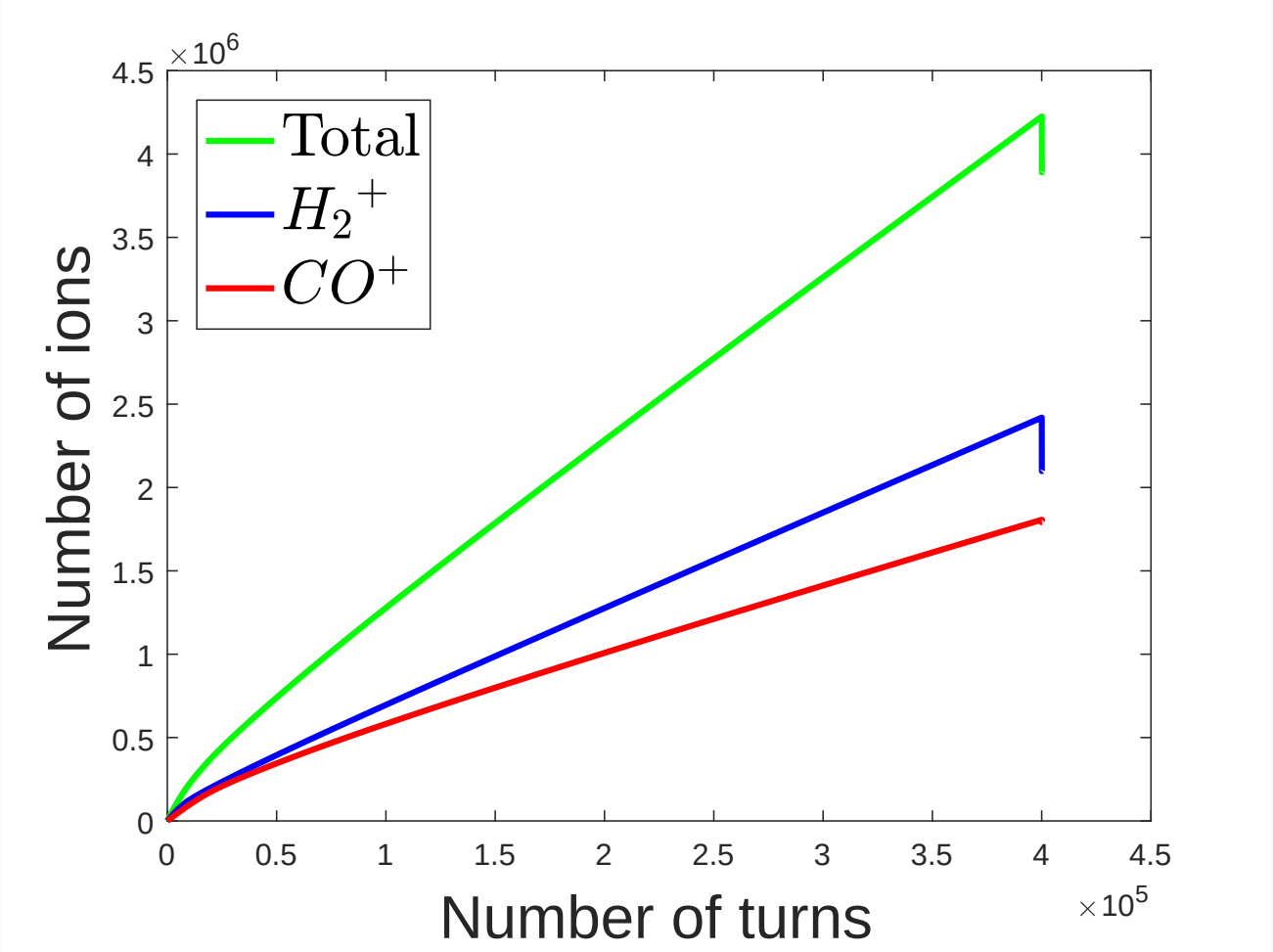

Figure 18: Number of ions CO^+ and $H_2{}^+$ during the first cycle and first small gap.

Second and further cycles

- N_a ions from the previous part are distribuited **non-uniformly**.
- $\varepsilon_a(n)$ is the clearing coefficient for such ions.

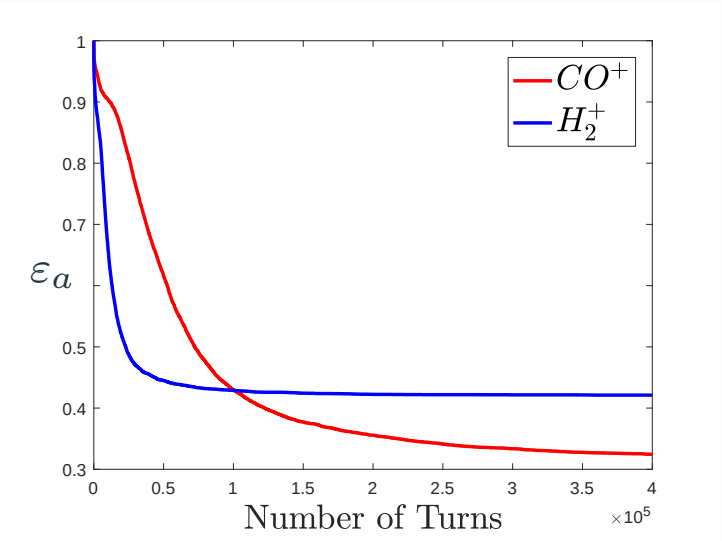

Figure 19: Clearing coefficient for the ions CO^+ and $H_2{}^+$ that were non-uniformly distributed along the ring.

- Yet we must add new ions N_{new} with the corresponding clearing coefficient $\varepsilon(n)$ for the **uniform** initial distribution.

Generalized formula for cycles

$$N_{ions}(n) = N_a \cdot \varepsilon_a(n) + N_{new} \cdot \int_0^n \varepsilon(z)dz, \quad n \in [0,\ n_{cycle} = 4 \cdot 10^5 \text{ turns}]. \tag{14}$$

First two cycles with small gaps

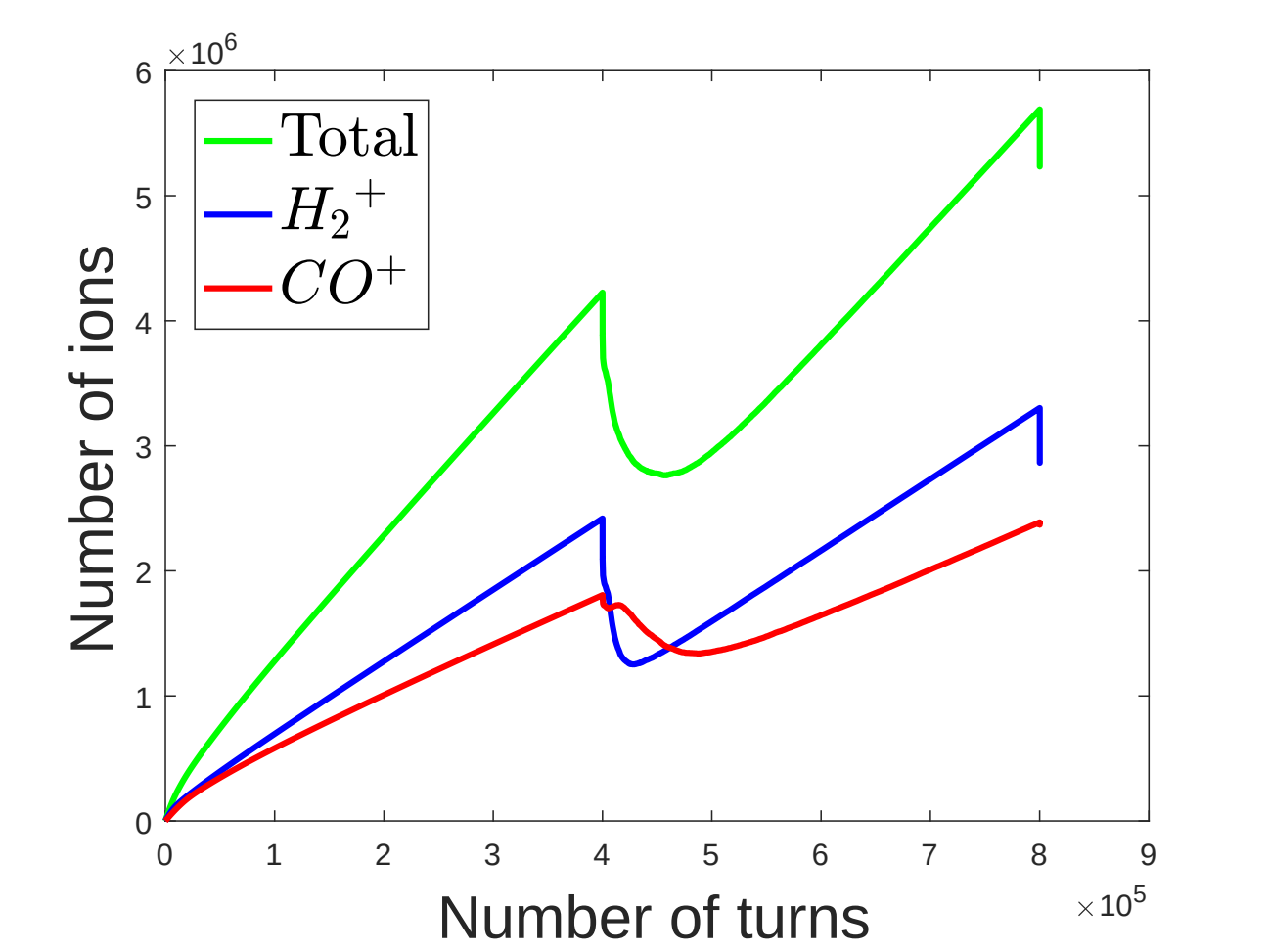

Figure 20: Number of ions CO^+ and $H_2{}^+$ during the first two cycles with small gaps.

Big gap ($4 \cdot 10^5$ turns without a bunch)

- Reliable cure against ions.
- Clearing coefficient $\varepsilon_{bg}(n)$.

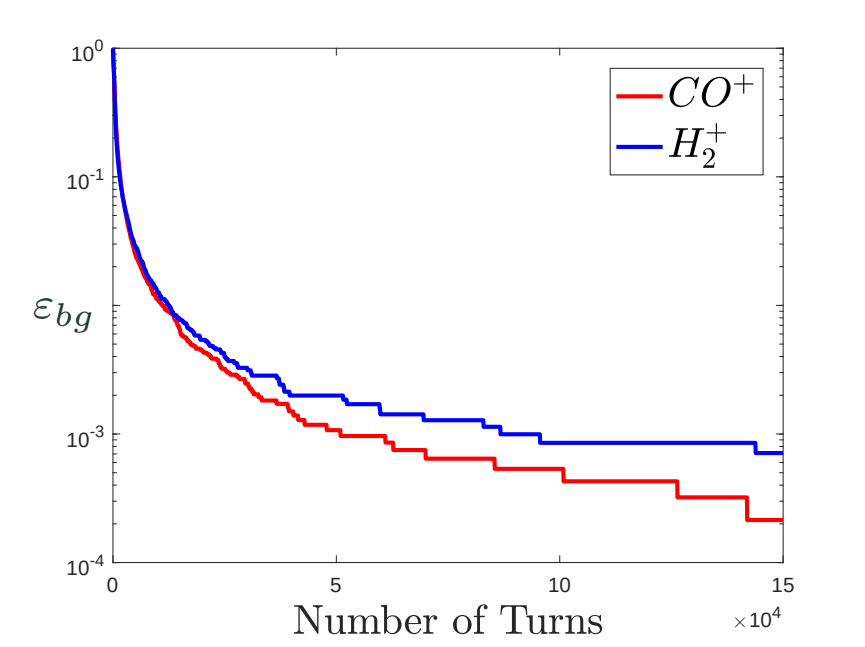

Figure 21: Clearing coefficient for the ions CO^+ and $H_2{}^+$ during the $1.5 \cdot 10^5$ turns without an electron bunch.

N_{ions} during the big gap

$$N_{ions}(n) = N_a \cdot \varepsilon_{bg}(n),$$
$$n \in [0,\ n_{bg} = 4 \cdot 10^5 \text{ turns}]. \quad (15)$$

Saturation

Summarizing formula

$$\begin{cases} \text{Cycle: } N_{ions}(n) = N_a \cdot \varepsilon_a(n) + N_{new} \cdot \int_0^n \varepsilon(z)dz, \ n \in [0, \ n_{cycle}], \\ \text{Small gap: } N_{ions}(n) = N_a \cdot \varepsilon_{sg}(n), \ n \in [0, \ n_{sg}], \\ \text{Big gap: } N_{ions}(n) = N_a \cdot \varepsilon_{bg}(n), \ n \in [0, \ n_{bg} = n_{cycle}]. \end{cases} \tag{16}$$

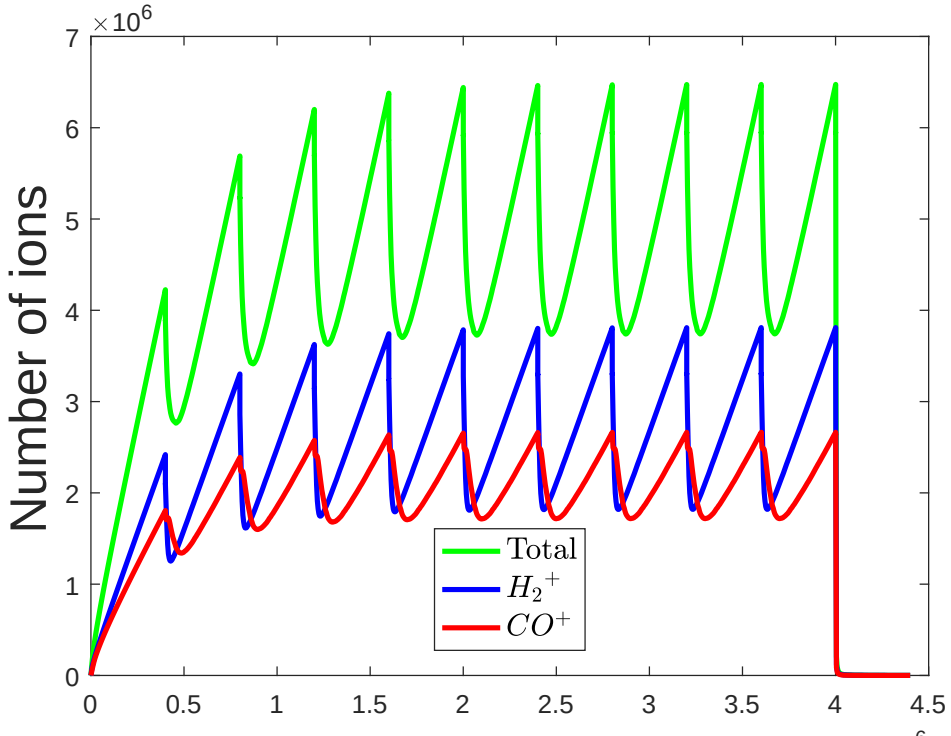

Figure 22: Number of ions CO^+ and $H_2{}^+$ during the first 10 cycles with small gaps and final big

Without electrodes

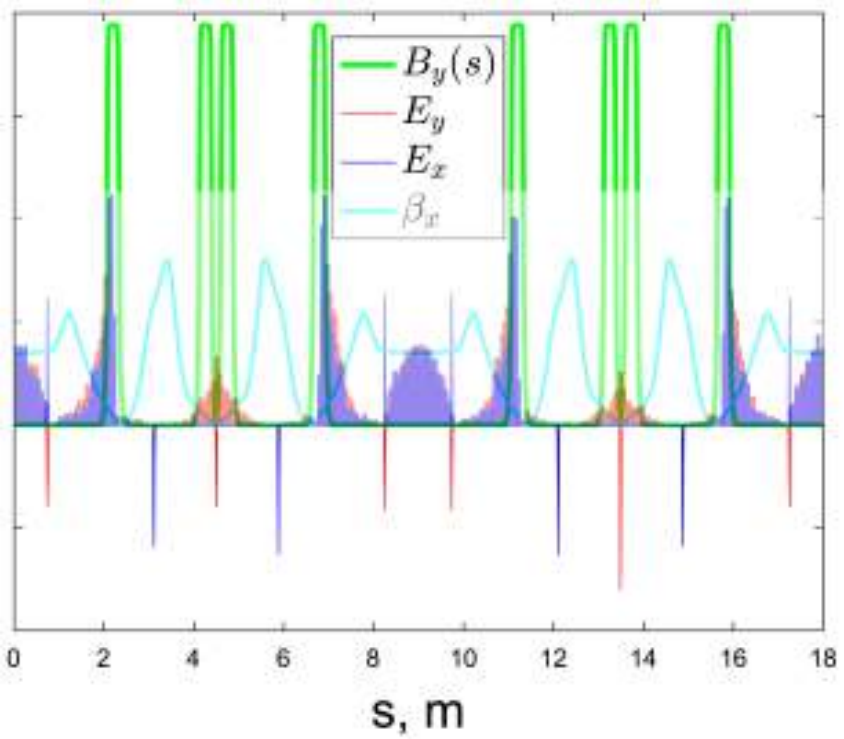

Figure 23: Final distribution of ions **WITH** electrodes with the behaviour of B_y, $E_{x,y}$, β_x.

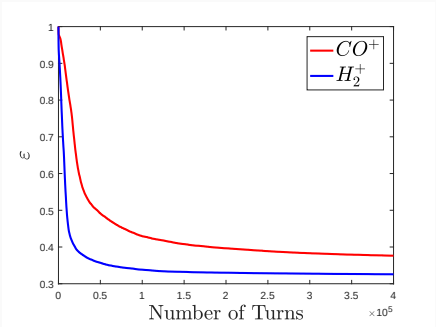

Figure 24: Clearing coefficient for the ions CO^+ and $H_2{}^+$ that were initially uniformly distributed along the ring. **With electrodes.**

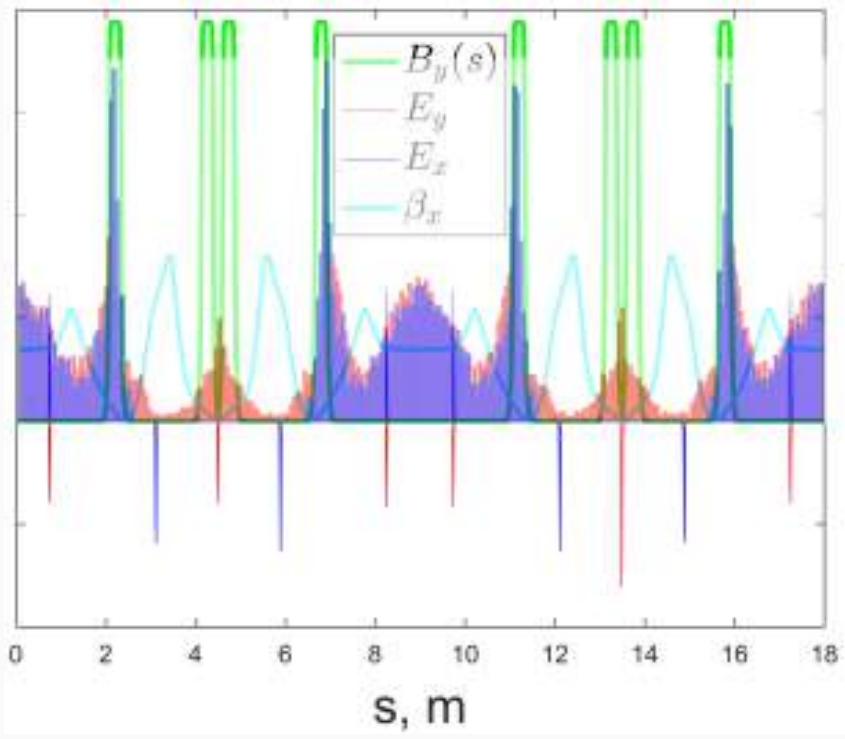

Figure 25: Final distribution of ions **WITHOUT** electrodes with the behaviour of B_y, $E_{x,y}$, β_x.

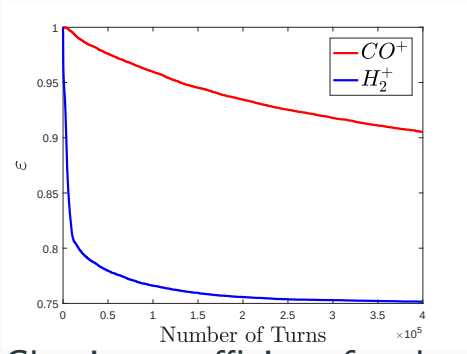

Figure 26: Clearing coefficient for the ions CO^+ and $H_2{}^+$ that were uniformly distributed along the ring. **Without electrodes.**

Without electrodes

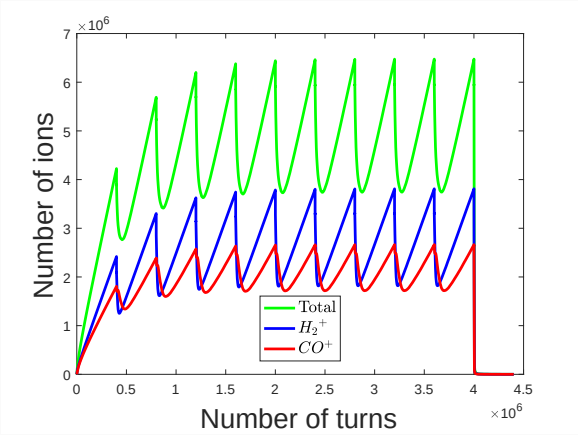

Figure 27: Number of ions CO^+ and $H_2{}^+$ during the first 10 cycles with small gaps and big gap at the end. **With electrodes.**

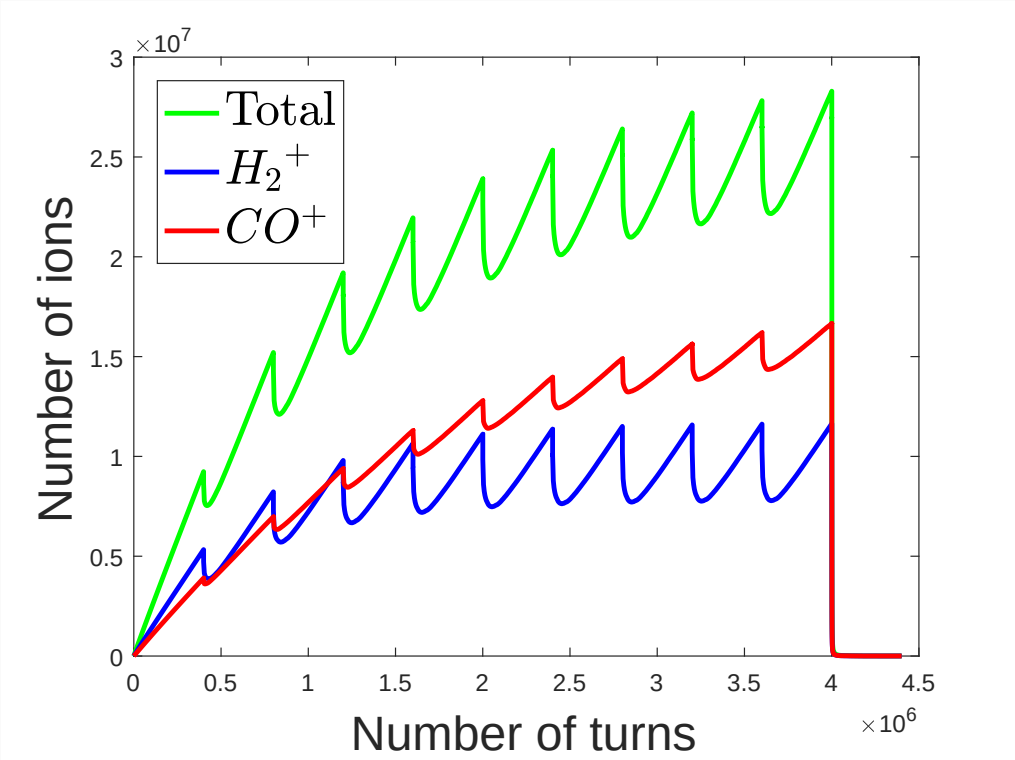

Figure 28: Number of ions CO^+ and $H_2{}^+$ during the first 10 cycles with small gaps and big gap at the end. **Without electrodes.**

Without small gaps

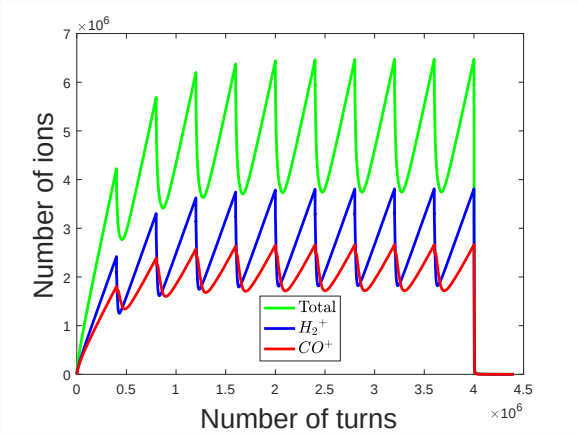

Figure 29: Number of ions CO^+ and $H_2{}^+$ during the first 10 cycles **with small gaps** and big gap at the end.

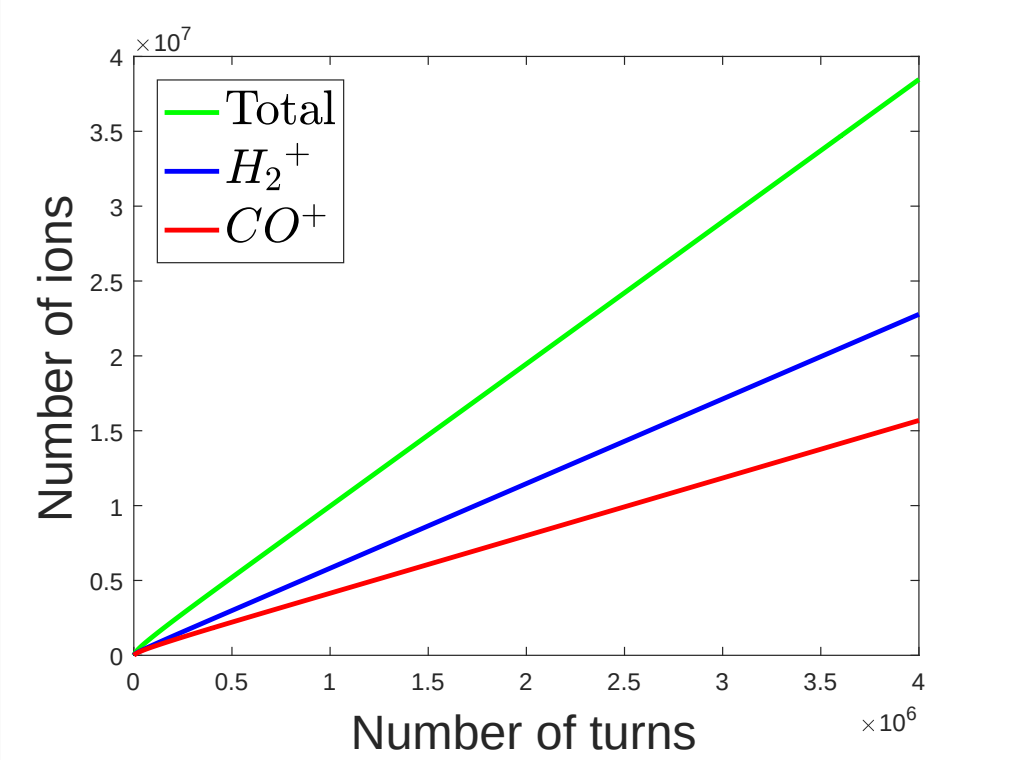

Figure 30: Number of ions CO^+ and $H_2{}^+$ during the first 10 cycles. **Without small gaps.**

Conclusions

- Interaction of the residual gas with beam was considered. However, only for single ionization.
- Ion tracking with the beam-ion interaction, ion movement in dipole and quadrupole magnetic fields was implemented.
- Quadrupole influence is almost negligible for the residual ions.
- 1.5 or 2 times increase of the electrode field did not change our results. Yet the placement of the electrodes in the ThomX ring should be investigated.
- Small gaps are important for the ion clearing. The longer gap, the better.
- Multi-ionization of the residual gas requires additional research.

Thank you